

05-92
242633

N90-13307

'SUMER' - SOLAR ULTRAVIOLET MEASUREMENTS OF EMITTED RADIATION

K. Wilhelm¹, W.I. Axford¹, W. Curdt¹, A.H. Gabriel², M. Grewing³, M.C.E. Huber⁴, S.D. Jordan⁵, P. Lemaire²,
E. Marsch¹, A.I. Poland⁵, A.K. Richter¹, R.J. Thomas⁵, J.G. Timothy⁶, and J.-C. Vial²

¹ Max-Planck-Institut für Aeronomie; ² Institut d'Astrophysique Spatiale;
³ Astronomisches Institut, Tübingen; ⁴ Space Science Department of ESA/ESTEC and Institut für Astronomie, Zürich;
⁵ NASA/Goddard Space Flight Center; ⁶ Center for Space Science and Astrophysics, Stanford

ABSTRACT

With SUMER - *Solar Ultraviolet Measurements of Emitted Radiation* - we will study flows, turbulent motions, waves, temperatures and densities of the plasma in the upper atmosphere of the Sun. Structures and events associated with solar magnetic activity will be observed on various spatial and temporal scales. This will contribute to the understanding of coronal heating processes and the solar wind expansion. The instrument will take images of the Sun in EUV light with high resolution in space, wavelength and time. It can provide a spatial resolution of 1.2 arcsec and its spectral resolving power is characterized by a $\lambda/\delta\lambda$ of up to 4.0×10^4 , where $\delta\lambda$ corresponds to the pixel size. Spectral shifts can be determined with sub-pixel accuracy. The wavelength range will extend from 500 to 1600 Å. The integration time can be as short as 1s. Information will be obtained on line profiles, shifts and broadenings, as well as on ratios of temperature- and density-sensitive EUV emission lines that are formed at temperatures between 10^4 and 2×10^6 K.

Keywords: EUV emission lines, coronal heating, solar wind acceleration.

1. SCIENTIFIC OBJECTIVES

1.1 Perspective

High-accuracy spectral imaging in EUV emission lines will allow us to study many physical parameters of the solar atmosphere: plasma density and temperature, abundances of species, velocity fields, topologies of the plasma structures, their time evolution and dynamics. Such measurements are of prime importance for the following areas of science:

- Solar physics. A determination of these parameters is essential for discriminating between different coronal heating mechanisms. Knowledge of the local energy distribution will give insights into the source regions of the solar wind and its acceleration.
- Stellar physics. Many stars have coronae and winds. Their physical interpretation is crucial to our understanding of stellar angular momentum loss and evolution. The Sun is the only star where theoretical concepts of coronal heating and wind generation mechanisms may be tested observationally by resolving the plasma structures.
- Plasma physics. The topology of the solar plasma is defined by magnetic fields, which are rooted in the photosphere and convection zone. This natural plasma environment accessible to detailed observations offers the long-sought opportunity to improve our understanding of astrophysical and laboratory plasmas.
- Solar-terrestrial relationship. The Earth, in common with the

other planets, is immersed in the solar wind and radiation field. The terrestrial atmosphere responds dynamically to photons and particles expelled from the Sun.

1.2 Physical Processes in the Solar Transition Region and Low Corona

1.2.1 Coronal heating. The outer solar atmosphere has often been described as a quiet plasma background, where temperature and density vary as a function of height, within which are embedded more complex features, such as active regions, prominences, loops and bright points. In these descriptions the temperature rises abruptly from values of about 10^4 K in the chromospheric layer, which occupies the first 2×10^3 km above the photosphere, to values in excess of 10^6 K in the corona, across a transition region only a few hundred kilometres thick. One would, however, expect a temperature decrease with distance from the photosphere unless non-radiative heating takes place. Thus, the existence of a chromosphere and a corona requires a persistent energy input to compensate for radiative and conductive losses and for the solar wind expansion. The relative importance of the processes proposed to be responsible for this energy input is a matter of debate. However, as pointed out by Athay (Ref. 1), the presence of any non-radiative mechanical heating mechanism should manifest itself by fluctuations, which may be detected by optical means in terms of line broadenings and Doppler shifts.

1.2.2 Solar wind acceleration. The thermal-pressure gradient mechanism proposed by Parker (Ref. 2), is inadequate to accelerate the solar wind to the high velocities observed in streams associated with coronal holes and may even be inadequate for producing the solar wind over the rest of the Sun. Thus, our current picture of the solar wind demands further acceleration mechanisms (Ref. 3-6) to explain the properties that have been measured at a distance beyond 0.3 AU from the Sun. Modern concepts of high speed solar wind acceleration hinge on the amount of wave energy available in the corona to drive the wind by wave pressure gradient forces, although it is also possible that the solar wind represents the accumulated effect of many small isolated acceleration sites.

1.2.3 Structure of the solar upper atmosphere. At the base of the corona small and large inhomogeneities are in a continuous state of fluctuation on time scales ranging from seconds to days and sometimes weeks. By confining plasma, the magnetic field plays a dominant rôle in permitting the large variety of physical conditions seen in coronal structures. In addition, the magnetic field may be responsible for both transporting and dissipating the

energy needed to maintain the plasma at coronal temperatures. In fact, although the non-thermal energy flux supplied at chromospheric levels in quiet regions and coronal holes is approximately the same (Refs. 7, 8), the non-thermal energy is converted predominantly into heat in the former case, whilst in the latter it is used in accelerating the solar wind.

1.3 Measurements Required

In order to understand the global balance of the inhomogeneous solar atmosphere, including the dynamics of the solar wind, we must understand the budget and transfer of mass, momentum and energy in the different structures of the chromosphere, transition region and lower corona. Therefore, we need to examine flows, oscillations and transient events and, at the same time, to investigate the plasma density, emission measure and temperature distribution.

We plan to study solar structures down to the 1-arcsec level with the help of emission lines in the wavelength range from 500 to 1600 Å covered by SUMER. Some of the lines observable in this range are shown in Fig. 1. This coverage has to be complemented at shorter wavelengths by the *Coronal Diagnostic Spectrometer* - CDS.

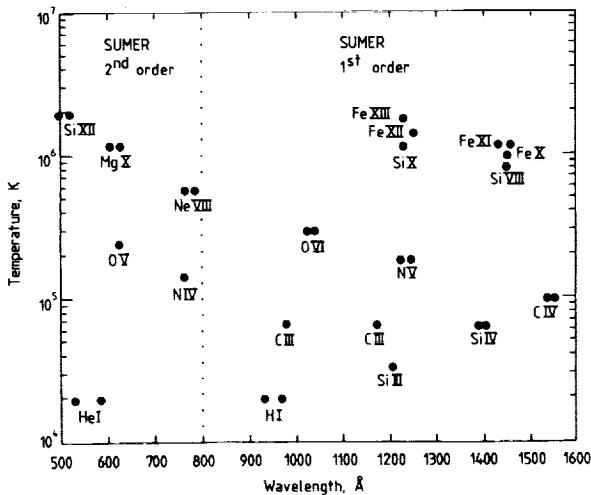


Fig. 1 Selection of emission lines in the SUMER wavelength range from 500 to 1600 Å

The desired temporal resolution depends on the lifetimes of the transient events. Wave activity represents the most demanding case and may require sampling times of about 1 s. The study of some other phenomena does not need such a high time resolution but a continuous time coverage. This is the case for the chromospheric network and its extension into the corona, for centres of activity as well as for the large-scale reconnection and loop torsions. Measurements of lifetimes, periodicities, and growth and decay times of these structures at different wavelengths would provide a better picture of the varying Sun. Ideally observing sequences should be performed over extended periods of time with no interruptions. For this reason SOHO in its halo orbit around the L1 libration point is an excellent platform from which to make such observations.

1.3.1 Techniques. The physical properties of the solar atmospheric structures and regions discussed above can be determined by the following techniques:

- Line profiles, shifts and broadenings. These measurements will give information about the dynamical phenomena in the solar

atmosphere. Line broadening in excess of the thermal widths may be caused by unresolved flows and/or wave activity or by actual turbulence.

- Line pair ratios. Atomic physics of excitation of highly-ionized species provides information on either the electron temperature T_e or the electron density N_e of the source from measurements of the intensity ratio of certain selected line pairs. The ratio of the emissivities for two optically-thin, allowed transitions excited from the same level is dependent on temperature T when the difference between the energies of the two transitions is of the order of kT . Ratios also become dependent on electron density, when metastable levels are involved (whose populations are largely determined by collisions) (Refs. 9–11).

1.4 SUMER Performance Characteristics

The SUMER instrument uses a single off-axis parabolic mirror with a collecting area of $S = 117 \text{ cm}^2$ as the primary telescope. In the diffraction limit, 80 % of the energy is encircled in 0.5 arcsec. A grating-spectrometer using normal-incidence optics will provide stigmatic spectra on 2-dimensional detectors with high resolution to resolve line profiles for small areas on the Sun.

The spectrometer covers the wavelength range from 500 to 1600 Å. The upper boundary was selected in order to include the C IV lines, but to avoid intense continuum radiation. The lower limit was set by the normal-incidence technique employed. The range from 500 to 800 Å will be observed in the 2nd order spectrum, whilst 800 to 1600 Å can be scanned in 1st order. The instrument simultaneously observes a spectral range of 40 Å in 1st order and 20 Å in 2nd order.

The effective equivalent surface of the instrument can be calculated from $A_\lambda = SR_{p1}R_{p2}R_{pm}E_gE_d$, where S is the collecting surface area of the telescope, R_{p1} , R_{p2} , R_{pm} are the mirror reflectivities, and E_g , E_d are the grating and the detector efficiencies (cf. Fig. 3). If we use the reflectance of SiC (Ref. 12) for all mirrors and assume the grating efficiency to be half the mirror reflectivity, we obtain a maximum effective collecting area of approximately 0.3 cm^2 for MgF_2 and 0.8 cm^2 for KBr detector coatings.

The pixel size of $25 \mu\text{m}$ in the spatial direction corresponds to an angular element of 1 arcsec or a distance of 700 km on the Sun. The spatial resolution thus achieved is adequate to study small-scale coronal loops and other structures and is compatible with the design goal of the spacecraft stability. The slit widths used for observations on the solar disk will be 0.5 or 1.0 arcsec. A wider slit with 4 arcsec can be selected for off-the-limb observations out to $1.5 R_\odot$. The low-scattering characteristics of a single mirror telescope will also permit observations in regions with strong gradients, such as coronal hole boundaries. The length of the slits will be between 25 and 300 arcsec. The spectral resolution can be characterized by a plate scale between 0.59 and $0.63 \text{ mm}/\text{Å}$ in the 1st order spectrum and double those values in 2nd order. With a pixel size of $25 \mu\text{m}$ in the diffraction direction, we thus obtain detected spectral elements of $\delta\lambda \approx 41 \text{ mÅ}$ and 20.5 mÅ , respectively. The parameter $\lambda/\delta\lambda$ characterizing the spectral resolving power varies between 1.9×10^4 and 4.0×10^4 as a function of the observing wavelength, where $\delta\lambda$ corresponds to the pixel size.

The velocity sensitivity of a line is a function of the total number of counts, the line width, the spectral element and the wavelength. By using a Gaussian line profile, only perturbed by statistical noise, we obtain the expected line shift sensitivity as a function of the total number of counts. This has been estimated for three cases plotted in Fig. 2, where $\Delta\lambda_D$ is the Doppler width. The velocity was derived from the wavelength shift by the Doppler formula $v_i = c(\lambda - \lambda_0)/\lambda_0$, where λ_0 is the nomi-

nal wavelength of a line. Other noise sources will also influence the sensitivity. We expect for many lines a useful range down to about 1 to 3 km/s with a position determination of spectral features at sub-pixel accuracy.

Depending on the line intensity, a temporal resolution down to 1 to 3 s can be obtained. The time required for the instrument to step from one wavelength range to the next would be between 1 and 10 s.

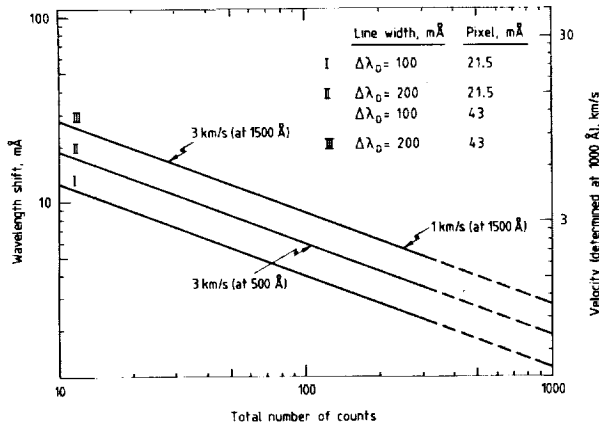


Fig. 2 Diagram showing the expected velocity sensitivity of SUMER as a function of the total number of counts in a line for different sets of parameters.

1.5 Lines for Dynamic and Diagnostic Studies

SUMER will primarily determine the characteristics of emitted radiation with the aim of deriving plasma parameters of the solar atmosphere from atoms or ions. It is thus essential to determine appropriate lines and line pairs. A particularly good coverage of the temperature range accessible to SUMER can be obtained at the scan mirror position shown in Table 1. The table implies a specific coating pattern on the detector, details of which still have to be studied.

Table 1: Selected lines for dynamical studies observable at a single wavelength scan position corresponding to a range from 1218–1258 Å in 1st order and 609–629 Å in 2nd order. Count rates expected are given for the full line and a spatial resolution element of 1 arcsec².

Atom or Ion	Temperature, T_e , K	Wavelength, Å	Counts/s		Photocathode
			Quiet	Plage	
C I	1.0×10^4	1253.40	15	95	KBr
N V	1.5×10^5	1242.80	72	942	KBr
Fe XII	1.8×10^6	1242.00		255	KBr
N V	1.5×10^5	1238.82	39	179	MgF ₂
O V	2.5×10^5	1218.35	3	33	MgF ₂
Mg X	1.1×10^6	625.20	5	38	KBr
		609.80	7	48	MgF ₂

Table 2 shows a selection of line pairs whose ratios are density or temperature dependent. The density ranges, over which the ratios are useful, are indicated, as are the temperatures of maximum abundance. The intensities of these lines, given in terms of predicted count rates, are also shown. Many pairs can simultaneously be observed using the same scan mirror setting. Some require a scan mirror motion with a corresponding deadtime.

2. CORRELATIVE STUDIES PLAN

The scientific objectives outlined in Section 1 call for a co-ordinated approach in the study of the coronal heating and solar wind generation processes. SUMER has very high performance

characteristics in spatial and spectral resolution for a restricted wavelength range. This implies a relatively small intrinsic field-of-view and a narrow spectral window that can be covered simultaneously. The contribution of SUMER to the understanding of the solar atmosphere and its dynamics will thus be greatly enhanced by co-ordinating its measurements with related observations made on SOHO or elsewhere.

We plan to co-operate with the *Coronal Diagnostic Spectrometer* - CDS in a very close way. This instrument extends our wavelength range to shorter values, providing the opportunity to measure additional line ratio pairs for density and temperature determinations. For the O VI ion line pair, for instance, that can provide temperatures in the wide range from 3×10^5 to 1×10^6 K, one line at 1032 Å falls into the prime window of SUMER whilst the other one at 173 Å can only be observed by grazing incidence techniques.

One of the problems that has to be solved in co-ordinating the observations of more than one instrument in space and time is the relative co-alignment. SUMER will have a Sun camera to facilitate such an alignment. It will also be important to define a standard co-ordinate system that will be used by all experiments.

The narrow instantaneous field-of-view of SUMER will also lead to the requirement of receiving in real-time or near real-time information from the *Extreme Ultraviolet Imaging Telescope* - EIT which has a wider view angle for selecting appropriate areas on the Sun or in the inner corona. This information is also necessary for a proper definition of the boundary conditions within which the spatially restricted observations have to be interpreted. For magnetic studies, magnetograph observations obtained on the ground and by the *Michelson Doppler Imager* - MDI will be required as well. The SUMER team will use the long non-station pass periods of SOHO to perform imaging activities of the full solar disk. At the beginning of an acquisition slot, a data dump followed by a quicklook display could provide information on interesting areas for SUMER, CDS and other instruments.

The low level of scattered light in the SUMER instrument allows us to perform a radial velocity analysis by using the Doppler dimming technique for the same lines as the *Ultraviolet Coronal Spectrometer* - UVCS, but at lower heights. The onset of accelerated flow at the base of the corona can thus be studied. The *White Light Coronagraph* - LASCO would provide the density diagnostics necessary for the above analysis.

We also hope to co-operate with solar wind particle experiments that measure the in-situ characteristics of the solar plasma at 1 AU. Of particular interest would be the composition and the charge state of the solar wind ions as determined by the *Charge, Element and Isotope Analysis System* - CELIAS.

3. DATA REDUCTION AND ANALYSIS PLAN

On-board data selection, compression and reduction methods are an essential aspect of this experiment. The limited transmission rate of SOHO not only requires these schemes, but also the fact that the original data rate would give 2×10^{14} bits over a mission time of 2 years.

SUMER provides spectroheliograms in many lines and of variable spatial extent. The high spectral resolution permits the measurement of spatial distributions of plasma velocity and turbulence fields. Temperature and density distributions can be obtained by observing in more than one line. All of these data can be stored and displayed as images of 2-dimensional arrays with the relevant parameters coded appropriately.

In parallel with the real-time data evaluation, investigators, associate scientists and guest investigators will perform preliminary data analysis tasks, using the capabilities provided by the Exper-

Table 2: Selected line pairs useful for density or temperature diagnostic studies. The expected count rates using a KBr photocathode are given for the full line and a spatial resolution element of 1 arcsec^2 . Dead times are required for wavelength range variations.

Ion	Wavelength, Å	Density	Temperature	Counts/s		Dead-time, s
		N_e , electrons/cm ³	T_e , K	Network	Plage	
S X	1213/1196	$2.0 \times 10^8 - 2.0 \times 10^{10}$	1.2×10^6	9/2	46/16	0
C III	1176/977	$1.0 \times 10^9 - 1.0 \times 10^{10}$	7.0×10^4	178/305	1950/2070	2
O V	760/630	$1.0 \times 10^9 - 1.0 \times 10^{10}$	2.5×10^5	7/52	20/100	3
Si III	1312/1301	$1.0 \times 10^9 - 1.0 \times 10^{11}$	3.5×10^4	-/7	31/85	0
Mg X	625/609		$3.0 \times 10^5 - 1.5 \times 10^6$	5/11	38/69	0
O IV	790/554		$8.0 \times 10^4 - 2.0 \times 10^5$	42/6	69/9	5
N III	991/686		$< 7.0 \times 10^4$	46/5	203/7	4
O VI	1032/173		$3.0 \times 10^5 - 1.0 \times 10^6$	334/*	1730/*	-

* Coronal Diagnostic Spectrometer - CDS observations

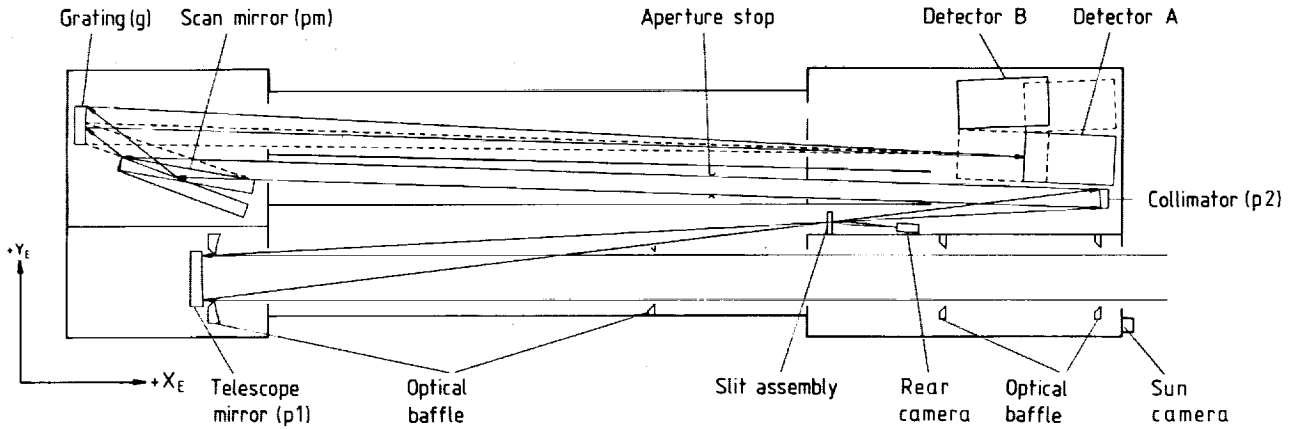


Fig. 3 Schematic optical design of SUMER. The scan mirror and the detectors have been drawn in the extreme positions of their scan ranges. Also shown is the experiment co-ordinate system.

iment Operations Facility (EOF). A science analysis team will co-ordinate the data collected not only from SOHO experiments, but also from simultaneous ground-based observations and will prepare scientific requirements for future operations.

4. TECHNICAL DESCRIPTION

4.1 The SUMER Instrument: An Overview

The main objective of the SUMER measurements, namely to obtain high spectral and spatial resolution images of the solar disk and the inner corona, favours a normal incidence telescope followed by a spectrometer using the same technique. High contrast requirements, furthermore, drive the design to a single off-axis primary telescope mirror with low light scattering characteristics. This eliminates at the same time solar flux concentrations on a secondary mirror and thus reduces the danger of potential sensitivity deteriorations. Chemical-vapour-deposited silicon carbide - SiC(CVD) on a SiC substrate appears to be the best material for the optics in terms of optical quality, UV reflectivity and mechanical and thermal properties. Its reflectance is greater than 40 % in the wavelength range from 600 to 2000 Å with a maximum of 50 % near 1600 Å and is, therefore, suitable for observations above 500 Å and below the intense solar continuum.

The telescope mirror can perform both the instrument pointing in a range of $\pm 30 \text{ arcmin}$ about two perpendicular axes and the scan motion required to achieve images of the Sun. This allows us to mount the instrument in a fixed position on the spacecraft and thus provides great simplifications in the design as well as in operational constraints. This scheme, however, has the disadvantage that the path of rays inside the instrument is not constant for different viewing directions. In order to minimize calibration complexity, we selected a design that leads to a constant path of

rays in the spectrometer area with a well-defined aperture stop.

One of the main difficulties in our EUV range lies in an efficient detection system. It has to be an open device and yet should not be sensitive to visible light. We selected a MAMA (Multi-Anode Microchannel Array) detector for the prime detector as it fulfils most of our requirements. The complexity of the detector and its paramount importance for the operation of SUMER led to the conclusion that a single detector assembly would be an unacceptable risk, in particular, as the KBr coating required for part of the detector has to be protected by a hermetic seal during ground and launch operations. A second detector assembly of identical design, but without sensitive coating and seal, was therefore included. It would have less sensitivity at longer wavelengths and, because of its off-axis mounting position, a slightly deteriorated resolution.

The on-board experiment control and data handling requirements led to a design with 2 to 3 transputers supported by image memories and mass storage devices. The processors will be partially reprogrammable to implement control and data handling schemes that evolve during the SUMER operation period. The total mass and power requirements of the instrument are 91 kg and 37 W, respectively (89.2 kg and 35 W are agreed with ESA in the Experiment Interface Document, EID Part B). The nominal telemetry rate will be 10.5 kbit/s. High and low bitrate modes are also under study in order to optimize the telemetry requirements of several experiments.

EUV instrumentation exposed to the full solar flux is very sensitive to any type of chemical or particulate contamination. A cleanliness programme will thus be a major effort within the SUMER product assurance activities. The telescope and the spectrometer will be housed in a tight case (that would at the

same time serve as optical bench) and a door will be included in the design. There will still be the need for nitrogen purging, as it will be impossible to develop a vacuum-tight system within the given mass constraints. SUMER will not contain any consumables, and consequently its life is in principle not limited to a certain time span. There are, however, a few aspects that may limit its effective life. These are the total number of counts of the microchannel plate detectors and the run times of the various mechanisms. We will establish upper limits for the duration of safe life of these devices in space. On the basis of these numbers, we will allocate not more than half of the available resources to the first year of operation and not more than a quarter to the second year. Careful planning of the observations will substantially reduce the load on critical items.

4.2 Detailed Description of the Instrument

4.2.1 Optical design. The optical design shown in Fig. 3 is based on well-known optical components: two off-axis parabolic mirrors, a plane mirror and a spherical concave grating, all made out of SiC(CVD). A 4.5° off-axis parabola as telescope mirror with a focal length of 1.3-m images the Sun on the spectrometer entrance slit. Behind the slit an off-axis parabola having a focal length of 0.4 m collimates the beam issued from the slit. The parallel beam is deflected by a plane scan mirror onto a spherical concave grating, which diffracts the selected wavelength range on its normal (Wadsworth mount). The 2-dimensional detector located in the focal plane of the concave grating collects the monochromatic images of the spectrometer entrance slit. The slit dimensions therefore determine the spatial characteristics of the images and the detector size in the diffraction direction limits the spectral range that can be observed simultaneously. The coverage of the full spectral range of the instrument requires a wavelength scan. The telescope mirror can be directed to any target within a $1 \times 1\text{-deg}^2$ solid angle centred at the Sun by a rotation around its focus. This can be accomplished in steps of 0.76 arcsec or half steps of 0.38 arcsec without compromising the high-angular image quality of 0.5 arcsec on the entrance slit of the spectrometer. The actual field-of-view thus achieved is large enough to allow for some compensation of misalignments between SUMER and the spacecraft optical reference and the other coronal experiments whilst maintaining the capability to scan the solar disk and the inner corona out to at least $1.5 R_\odot$ in all directions. The effective resolution is the convolution of the image quality (0.5 arcsec), the slit width (1 arcsec for most of the observing modes) and the spacecraft pointing jitter ($\pm 0.5\text{ arcsec}$). We obtain 1.5 arcsec . For very bright lines, we can use the 0.5 arcsec slit and achieve an effective spatial resolution of 1.2 arcsec . Calibration of the pointing mechanism and checks of the image quality are made with the help of a camera located behind the slit through solar limb detection in diffracted light. The focal plane detector can also provide information on the optimal focus adjustment by observing the solar limb or other features with high contrast. The wavelength scan is carried out by a rotation of the plane mirror, thereby modifying the angle of incidence i on the grating, and a linear adjustment of the monochromatic focal distance f_λ . The wavelength diffracted onto the grating normal is given by $\lambda_n = (d \sin i)/m$, where m is the observing order and $d = 278\text{ nm}$ is the grating constant for a 3600 grooves/mm grating.

4.2.2 Focal plane design. The grating with a radius $r = 3.2\text{ m}$ has a focal distance and a plate factor in the first order spectrum varying with wavelength from about 1640 mm and $0.59\text{ mm}/\text{\AA}$ at 800 \AA to 1760 mm and $0.63\text{ mm}/\text{\AA}$ at 1600 \AA . Together with the focal length of the collimator of 0.4 m , we obtain magnification factors of 4.1 to 4.4 in the spatial domain. The configuration is stigmatic within a large field. The resolution is better than $43\text{ m}\text{\AA}$ and 0.5 arcsec in the $40\text{-}\text{\AA} \times 300\text{-arcsec}$ field chosen in the

first order. Outside this field, the image curvature combines with astigmatism to give two foci on the corresponding tangential and sagittal focal surfaces. An angular resolution of 2.5 arcsec along the monochromatic slit image will be obtained at 7-cm distance from the grating axis in the dispersion direction. The prime detector having a field of 360×1024 pixels will be positioned on the grating axis. The microchannel plate (MCP) of this detector is coated with MgF_2 in its short-wavelength portion and with KBr in the long-wavelength range. Consequently it requires a door assembly for ground and launch operations. The secondary detector will only have a MgF_2 coating. It will be positioned 7 cm off the grating axis in the dispersion direction.

4.2.3 Structure of telescope and spectrometer. Due to the multiple-folded path of rays in the instrument, the optical components are grouped towards its front and rear ends. These components can therefore be mounted inside two box-like substructures connected by a stiff but lightweight spacer section as shown in Fig. 4. This design presents a clean and smooth metallic inner surface required by the sensitive EUV optics and avoids contamination and structural deformation caused by outgassing effects. The structure is utilized both as the optical bench and housing for the instrument. The inside of the housing will be bare aluminium. The interface to the spacecraft is via thermally isolating isostatic mounts. The instrument carries a radiator of 1400 cm^2 for cooling the primary mirror.

4.2.4 Mechanisms. Six mechanisms will be required for the operation of SUMER. Two of them are described here in some detail.

4.2.4-1 Entrance door. Since this mechanism carries the risk of a single point failure of the whole instrument, its design has to include a redundant way of opening the entrance aperture. The door is opened by a stepper motor. In case of malfunction of this drive, the underlying annular frame is released by a pyrotechnical device and rotated back together with the door.

4.2.4-2 Telescope pointing. The mirror raster system will combine the coarse pointing and the high-resolution scan. In order to maintain the optical quality of the image on the entrance slit, the mirror will not only be tilted (which would move the paraboloid axis off the slit), but moved around on a spherical surface centred on the slit ($R =$ apparent focal length of off-axis mirror). This spherical motion is implemented as the superposition of two orthogonal circular motions. For small angles ($\pm 0.5\text{ deg}$), the circular motion can be approximated by a displacement and a tilt of a bar guided by its ends on a pair of rails set at an angle α . A circular motion with a radius of curvature R will approximately be achieved when $\tan(\alpha/2) = L/(2R)$, where L is the length of the bar. By ray tracing computations, it can be shown that the image quality on the spectrometer entrance slit is better than 0.5 arcsec within the $1 \times 1\text{deg}^2$ raster range.

4.2.5 Electronics system. The detector data are transferred in digital format to an image memory. It has two independent memory planes, one of which is used for accumulating the detector output whilst the other is read out. The accumulation results in a 2-dimensional image with a spatial and a spectral dimension. Two processors, the Experiment Control Processor (ECP) and the Signal Processing Unit (SPU), are used for control and data processing. They are functionally interchangeable. This allows an emergency mode to be selected where each processor could perform both its own tasks and those of the other one. The processors could also be interchanged in certain other failure modes. The operating memories of both the ECP and the SPU will be kept alive by a constantly powered line from the spacecraft. They will partly be adjustable by programme changes via ground command sequences. Programme changes of the on-board software will be made on the basis of actual data received and on the science evaluation with a view to enhancing the science information return within the fixed telemetry allocation. The mass memory

5. Parker E N 1983, Magnetic neutral sheets in evolving fields. II. Formation of the solar corona, *Astrophys J* 264, 642-647.
6. Withbroe G L 1987, Acceleration of the solar wind as inferred from observations, *Proc of the Sixth International Solar Wind Conference*, Estes Park, Colorado, 23-28 August 1987, in (Eds) Pizzo V J, Holzer T E & Sime D G, Volume I, NCAR, Boulder, 23-48.
7. Gabriel A H 1976, Structure of the quiet chromosphere and corona, *Proc of the International Astronomical Union*, Nice 6-10 September 1976, in (Eds) Bonnet R M & Delache P, 'The Energy Balance and Hydrodynamics of the Solar Chromosphere and Corona', 375-504.
8. Withbroe G L & Noyes R W 1977, Mass and energy flow in the solar chromosphere and corona, *Ann Rev Astron Astrophys* 15, 363-387.
9. Gabriel A H & Jordan C 1969, Interpretation of solar helium-like ion line intensities, *Mon Not R astr Soc* 145, 241-248.
10. Malinovsky M 1975, New calculations of atomic data concerning E.U.V. lines of O V, *Astron Astrophys* 43, 101-110.
11. Dere K P & Mason H E 1981, *Spectroscopic diagnostics of the active region: Transition zone and corona*, in (Ed) Orrall F Q, 'Solar Active Regions', Colorado Assoc. Univ. Press, 129-164.
12. Choyke W J & Palik E D 1985, *Silicon Carbide (SiC)*, in 'Handbook of Optical Constants of Solids', Academic Press, Inc., 587-595.

